Pergamon

Welding in the World/Le Soudage dans le Monde. Vol. 37, No. 1, pp. 90–104, 1996

Elsevier Science Ltd
0043-2288/96 $15.00 + 0.00

0043-2288(95)00069-0

Fatigue strength of spot welded beams in high strength steels

by C. Lindgren, J. O. Sperle and M. Jonsson (Sweden)

Abstract

Fatigue tests have been carried out on non-load and load carrying spot welded beams in mild and high strength carbon steel (HSLA 350) as well as 18Cr9Ni 304 stainless steel sheet, a microalloyed steel and dual phase steel DOCOL 600 with approximately 15% martensite. Constant amplitude, spectrum loading tests as well as tests with occasional overloads have been performed at alternating bending loads, R = –1. The applicability of different fatigue strength prediction models for spot welded joints have been checked against the results from this investigation together with results from other investigations. Among the tested prediction models, based on FE analysis, fracture mechanics, rotational stiffness and local stress approaches, the local stress approach proposed by Maddox and LBF seem to give the best fatigue strength prediction for the shear tensile joints considered here.

Key words: *Fatigue strength; Spot welding; Mild steel; Stainless steels; Finite element analysis; Models; Microalloyed steels; Resistance welding; High strength steels; Dual phase steels*

Résumé

Des essais de fatigue ont été effectués sur des poutres soudées par points transmettant ou non des efforts en acier doux, en acier à haute résistance (HSLA 350), en acier inoxydable 18Cr9Ni 304, en acier microallié et en acier dual phase DOCOL 600 comportant environ 15% de martensite. Des essais à amplitude constante, avec spectre de charge ainsi que des essais avec des surcharges occasionnelles ont été effectués avec des charges de flexion alternées, R = –1. L'applicabilité des différents modèles de prévision de la résistance à la fatigue pour les joints soudés par points a été vérifiée par rapport aux résultats de cette étude et d'autres études. Parmi les modèles testés, qui sont fondés sur une analyse par éléments finis, la mécanique de la rupture, la déformation angulaire du point et la contrainte géométrique locale, ce sont les méthodes de contrainte géométrique locale (autour du point et à l'intérieur du point) qui semblent donner les meilleures prévisions de résistance à la fatigue pour les joints sollicités en cisaillement dont il est question dans cette étude.

Mots clés: *Résistance à la fatigue; Soudage par résistance; Soudage par points; Acier doux; Acier inoxydable; Analyse par élément fini; Modèles; Aciers microalliés; Aciers à haute résistance; Acier dual phase*

IIS/IIW-1267-94 (ex. doc. XV-862-94/XIII-1553-94) Class A recommended for publication by IIW Commission XIII "Fatigue of welded components and structures" and Commission XV "Fundamentals of design and fabrication for welding" as the authors' own work.

The authors are research associates of the Materials Center.

Introduction

The use of high strength steel sheet, both coated and uncoated, is expected to increase in the years to come. When using these grades fatigue becomes a more dominant design criterion, and fatigue data on base materials and spot welded structures are needed to ensure an adequate fatigue life.

From tests on gas-metal arc welded specimens and shear loaded spot welded specimens we have learned that the fatigue strength of high strength steels determined under constant amplitude loading is not higher than that of mild steels.

Preliminary tests on tensile shear loaded spot welded specimens tested with occasional overloads did, however, indicate longer fatigue lifes for high strength steels, especially dual-phase steels, than for mild steels [1]. That holds also for non-load carrying spot welded specimens under constant amplitude loading [2] (Fig. 1). The reason for this somewhat unexpected behaviour for non-load carrying spot welds is probably that, in those specimens, the crack-like defect is not situated perpendicularly to the direction of loading and does not, therefore, cause the early start of crack propagation that normally makes the fatigue strength independent of base metal strength. This is also indicated by finite element analyses performed by Cooper and Smith [3].

In order to investigate which results are relevant to real structures, both non-load carrying and load carrying spot welded structural details were tested under constant amplitude loading, loading with occasional overloads and spectrum loading. Specimens in mild and high strength steel sheets were included. In the evaluation of the results, the load bearing capacity and its relation to the steel strength and spot weld nugget diameter as well as the influence of loading sequence are questions specifically addressed.

There are few general methods existing for prediction of the fatigue behaviour of spot welded structures. The applicability of some are, however, checked on the results from this investigation together with results from other investigations. Models based on FE analysis, fracture mechanics, rotational stiffness and local stress approaches are checked.

This report is a shorter version of a full paper on the fatigue strength of spot welded beams in high strength steels [4].

Experimental details

The sheet materials tested were a mild steel, SS 1147 (MS), of deep drawing type, a lean alloyed high strength dual-phase steel, DOCOL 600 (DP 600), with approximately 15% martensite, a high strength steel, DOCOL 350 YP (HSLA 350), microalloyed with Nb and a stainless steel, 304 (18Cr9Ni). The dual-phase grade was tested in two thicknesses, 0.8 and 1.0 mm, the other grades in 1.0 mm only. The chemical compositions and the

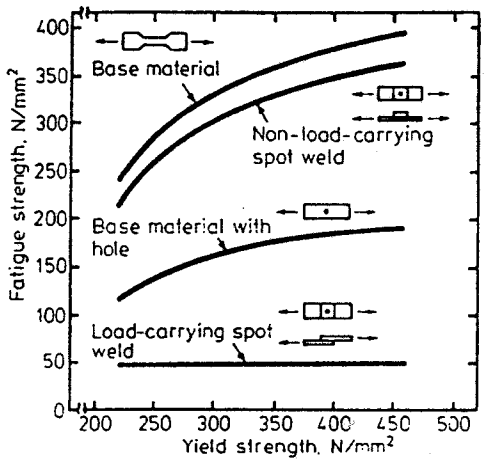

Fig. 1. A comparison between fatigue strength and yield strength for different notch cases for stress ratio $R = 0$. Number of cycles: $N = 2 \times 10^6$ [2]

mechanical properties of the steel grades tested are shown in Tables 1 and 2.

Fatigue tests were performed on non-load carrying (NLC) and load carrying (LCB) spot welded beams according to Figs 2(a) and (b).

The welding characteristics are shown in Table 3. The spot weld diameter was measured on almost all load carrying beams. The actual value of the spot weld diameter varied from 3.9 to 5.9 mm. The nominal value of the spot weld diameter is 5 mm. The fatigue tests were carried out under alternating four point bending loading with $R = 1$ [Fig. 2(a)]. Constant amplitude tests (CA), spectrum loading tests (SP) as well as tests with occasional overloads (OL) were performed. A 25 kN MTS testing machine was used. The test frequency was approximately 20 Hz. To avoid local load concentrations in the beam flanges the load was applied in the neutral layer of the beam.

For the spectrum loading a program was used which uses a reduced Markovian matrix for the generation of a random load sequence [4, 5].

Tests with occasional overloads were only performed on load carrying beams and the load sequence had one overload, twice the nominal load, every 25,000 cycles. The overloads were less than those causing permanent plastic deformation in the beams.

The criterion for final failure was set to a stiffness loss of 5% in the beam specimen. This failure criterion resulted in a final fatigue crack of 5–10 mm length. Almost all fatigue cracks started at the spot weld circumference.

Fatigue test results

All individual fatigue test results are given in Appendix I for non-load carrying and load carrying beams.

The stresses given in Appendix I and discussed further are nominal bending stresses referring to the centre line of the longitudinal welds, i.e. at a distance of 50 mm from the centre axis of the beam. The values given are stress amplitudes, S_a, which means that the total stress range is $S_r = 2 \cdot S_a$. For the constant amplitude tests the given stress is the basic stress level, i.e. the overload is twice that level. The stresses given for the spectrum tests are both the maximum stress, S_{amax}, in the spectrum and an equivalent stress, S_{eq}, calculated as follows:

$$S_{eq} = \left[\sum_{i=1}^{16} \frac{n_i \cdot S_{ai}^m}{N} \right]^{1/m} \quad (1)$$

where

n_i = number of cycles at stress level S_{ai} ($i = 1$–16)
S_{ai} = the actual stress level (MPa)
N = total number of cycles
m = slope of corresponding constant amplitude S–N curve.

S–N curves for non-load carrying beams are shown in Figs 3(a) and (b), where the spectrum loading results are expressed as S_{amax} and S_{eq}, respectively.

Earlier investigations [6] have shown that the fatigue strength of load carrying spot welds is greatly influenced by the spot weld

Table 1. Chemical composition of materials studied (weight %)

Steel grade	t (mm)	C	Si	Mn	P	S	N	Al	Nb	Cr	Ni
MA (A)	1.0	0.019	0.004	0.18	0.005	0.008	0.006	0.053	—	—	—
MS (B)	1.0	0.013	0.010	0.18	0.013	0.015	0.004	0.052	—	—	—
DP 600	0.8	0.093	0.160	0.74	0.073	0.006	0.008	0.067	—	—	—
DP 600	1.0	0.092	0.175	0.77	0.077	0.006	0.007	0.083	—	—	—
HSLA 350	1.0	0.054	0.213	0.55	0.008	0.007	0.008	0.061	0.030	—	—
18Cr9Ni	1.0	0.037	0.310	1.50	0.030	0.004	0.048	—	—	17.3	8.1

Table 2. Tensile properties of steels

Steel grade	t (mm)	Yield strength R_{eH} (MPa)	Tensile strength R_m (MPa)	Elongation A_{80} (%)
MA (A)	1.0	208	321	43
MS (B)	1.0	210	323	43
DP 600	0.8	386	646	20
DP 600	1.0	387	643	16
HSLA 350	1.0	420	482	24
18Cr9Ni	1.0	270*	649	61†

*0.2% proof stress.
†A5.

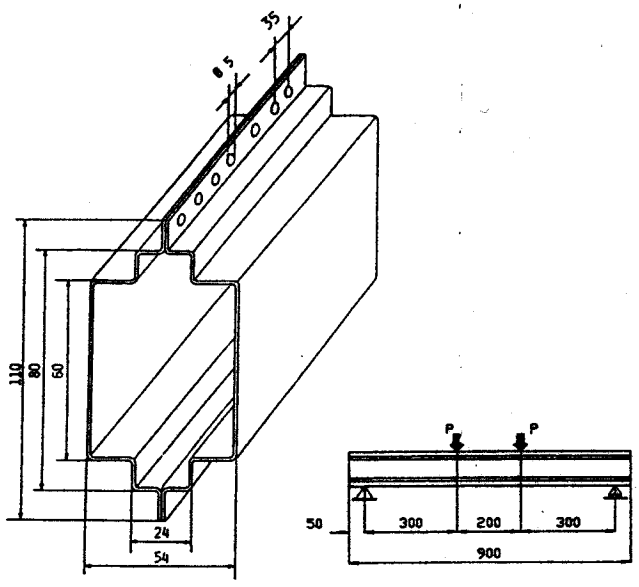

Fig. 2(a). Non-load carrying spot welded beam

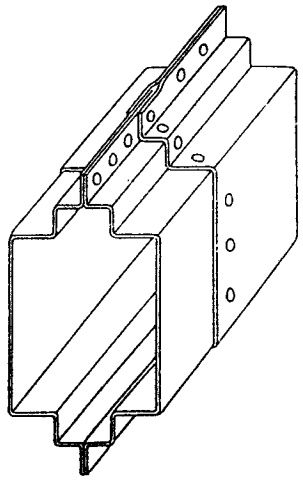

Fig. 2(b). Load carrying spot welded beam

diameter. All individual test results have therefore been recalculated to the same diameter, the metallographic investigation showing a large variation in diameter between different welding occasions. Finite element calculations on the load carrying beam and tests on small specimens [6] indicate that the influence of spot weld diameter on the fatigue strength can be described by:

$$S_d = S_{d0}\left(\frac{d}{d_0}\right)^{0.8} \quad (2)$$

where

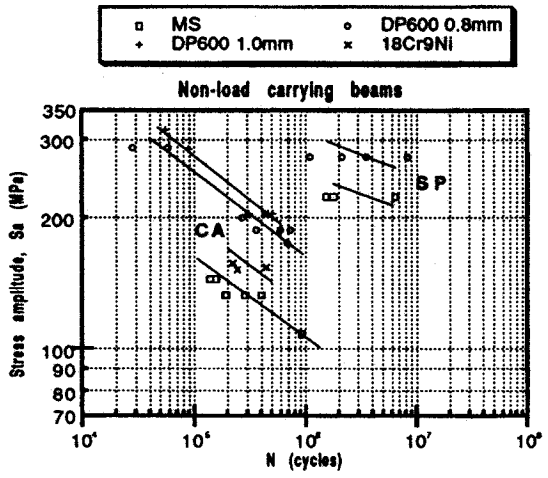

Fig. 3(a). *S–N* curves for non-load carrying beams, spectrum stress expressed as maximum stress, S_{amax}

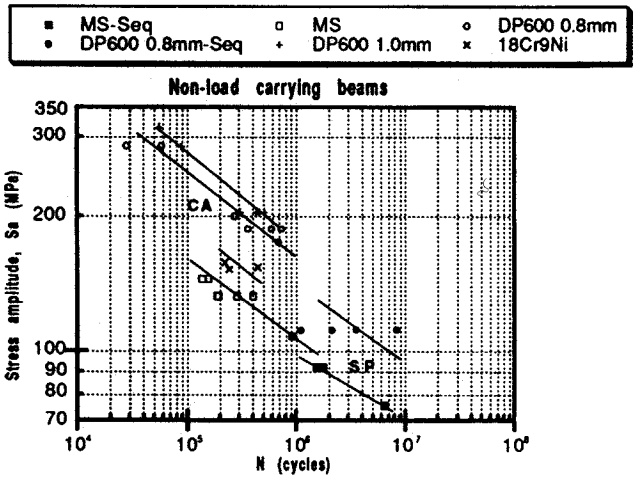

Fig. 3(b). *S–N* curves for non-load carrying beams, spectrum stress expressed as equivalent stress, S_{eq}

S_d = fatigue strength at actual diameter, d (MPa)
S_{d0} = fatigue strength at reference diameter, d_0 (MPa)
d = actual diameter (mm)
d_0 = reference diameter (mm).

The reference diameter chosen was d_0 = 5 mm. Such a correction of the fatigue strength results, to d_0 = 5 mm, decreased the scatter expressed as standard deviation in log N from 0.31 to 0.23.

The results from the constant amplitude tests and tests with occasional overloads for the load carrying beams are shown in Figs 4 and 5, respectively. The spectrum loading results for the

Table 3. Welding characteristics

Steel grade	t (mm)	Electrode diameter (mm)	Squeeze cycles*	Weld cycles	Hold cycles	Electrode force (kN)	Current (kA)
MS	1.0	5	10	10	10	2.5	8.2
DP 600	0.8	5	10	8	10	2.3	6.8
DP 600	1.0	5	10	10	10	2.5	7.2
HSLA 350	1.0	5	10	10	10	2.5	7.2
18Cr9Ni	1.0	5	10	10	10	2.4	6.9

*50 Hz.

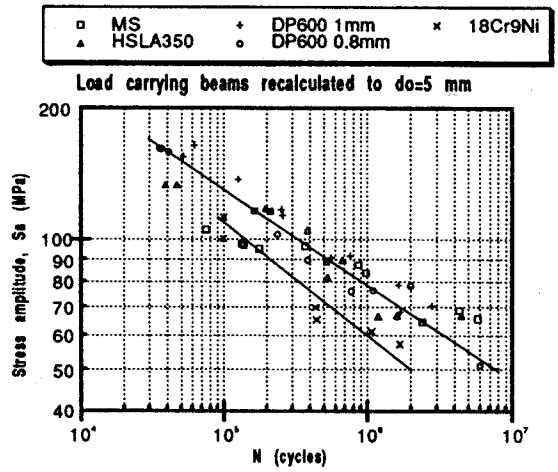

Fig. 4. *S–N* curves for load carrying beams tested under constant amplitude loading, results recalculated to $d_0 = 5$ mm

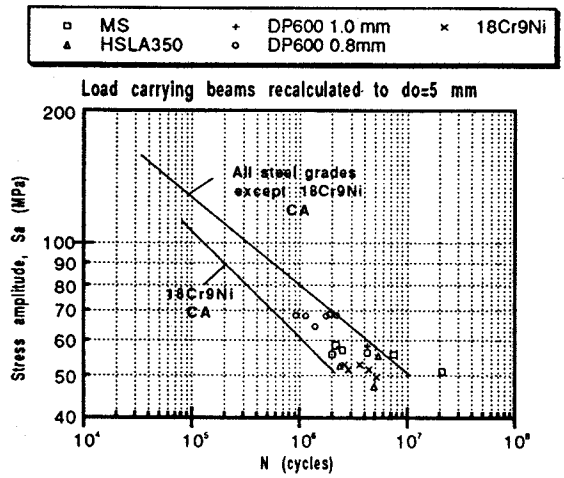

Fig. 6(b). Results from tests on load carrying beams, tested under spectrum loading, S_{eq}, shown together with mean *S–N* curves for constant amplitude tests

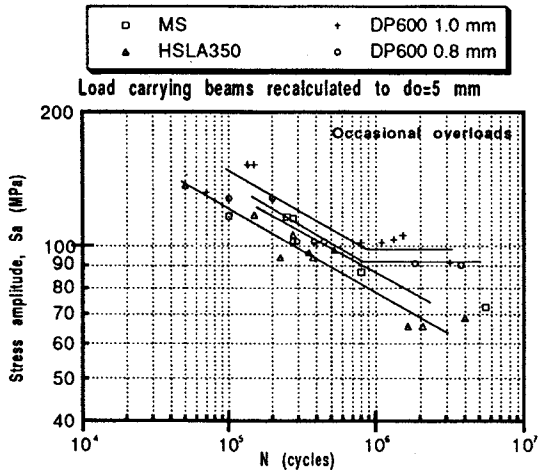

Fig. 5. *S–N* curves for load carrying beams tested with occasional overloads, results recalculated to $d_0 = 5$ mm

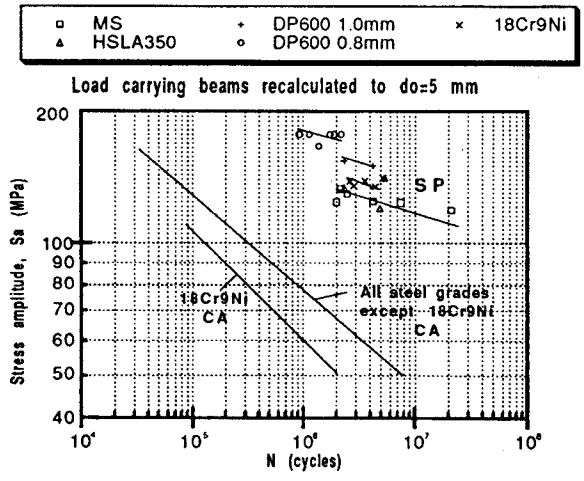

Fig. 6(a). Results from tests on load carrying beams, tested under spectrum loading, S_{amax}, shown together with mean *S–N* curves for constant amplitude tests

load carrying beams are shown together with the regression lines for constant amplitude results (Fig. 4) in Figs 6(a) and (b), where the spectrum loading results are expressed as maximum stress, S_{amax}, and equivalent stress, S_{eq}, respectively.

Discussion of fatigue test results

Mean values of the fatigue strength at $N = 10^6$ cycles are summarized in Tables 4 and 5 for non-load carrying beams and load carrying beams, respectively. Fatigue test results from spectrum loading only cover a limited life range and the fatigue strength at $N = 10^6$ cycles are therefore extrapolated values. The following discussion refers mainly to the fatigue strength at $N = 10^6$ cycles.

Fatigue strength

For non-load carrying spot welds one would expect it to be poss-ible to use the nominal tensile stress for comparison of the fatigue strength between different specimens and structural geometries.

A comparison between the fatigue test results for non-load carrying beams and small non-load carrying spot welds (Fig. 1) [2] shows, however, that the fatigue strength for the beams is 80% of that for small specimens. One reason for the somewhat smaller values for the beams could be the presence of secondary bending stresses due to "breathing", which can increase the stress by about 15% compared to the nominal stress.

The fatigue strength for load carrying beams is 1.2 times that of small load carrying spot welds [2, 6]. This higher fatigue strength for the beams could be explained by a higher rotational stiffness in the beams.

Tests on the small scale specimens [2, 6] have been performed at $R = 0$, and the fatigue strength have been recalculated to $R = -1$ using the rule of thumb S_a $(R = -1)/S_a$ $(R = 0) = 1.25$ in order to make the above comparison.

The effect of sheet thickness, for the beam type and thickness range tested, can be taken into account by considering the nominal stress. This is realized by considering the results for DP 600 in Figs 3 and 4.

Table 4. Summary of fatigue strength results at $N = 10^6$ cycles, non-load carrying beams

Steel grade	t (mm)	Loading condition	Yield strength (MPa)	Fatigue strength at 10^6 cycles S_a, S_{eq} (SP) (MPa)	S_{amax} (SP) (MPa)
MS	1.0	CA	209	107	—
		SP		(97)	(254)
D 600	0.8	CA	386	166	—
		SP		(129)	(321)
DP 600	1.0	CA	387	169	—
18Cr9Ni	1.0	CA	270*	(127)	—

*0.2% proof stress.
( )extrapolated values.

Table 5. Summary of fatigue strength results at $N = 10^6$ cycles, load carrying beams, $d_0 = 5$ mm

Steel grade	t (mm)	Loading condition	Yield strength (MPa)	Fatigue strength at 10^6 cycles S_a, S_{eq} (SP) (MPa)	S_{amax} (SP) (MPa)
MS	1.0	CA	209	80	—
		OL		87	—
		SP		(62)	(140)
DP 600	0.8	CA	386	77	—
		OL		92	—
		SP		(70)	(180)
DP 600	1.0	CA	387	84	—
		OL		98	—
		SP		(64)	(168)
HSLA 350	1.0	CA	420	78	—
		OL		78	—
		SP		(58)	(146)
18Cr9Ni	1.0	CA	270*	61	—
		SP		(57)	(153)

*0.2% proof stress.
( )extrapolated values.

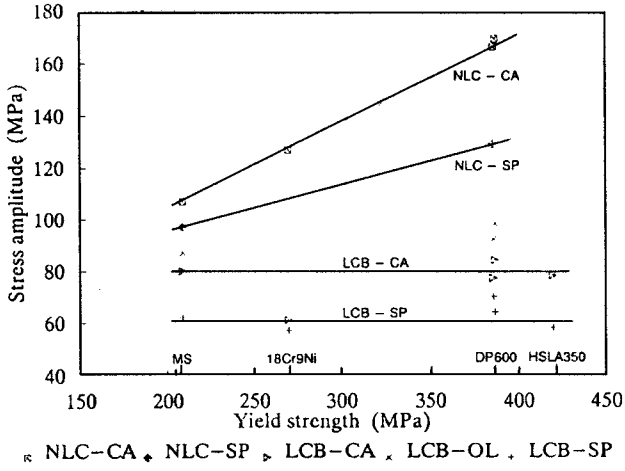

Fig. 7. Influence of yield strength on fatigue strength S_a, S_{eq} values according to Tables 4 and 5

Effect of steel strength

The influence of the yield strength on the fatigue strength for non-load carrying (NLC) and load carrying (LCB) beams tested under constant amplitude (CA) and spectrum (SP) loading is shown in Fig. 7.

The fatigue strength increases along with the base metal yield strength for NLC specimens tested under CA and SP loading. This behaviour was expected, considering the results for small shear tensile specimens, tested under CA loading, in Fig. 1 [2]. The increase in fatigue strength is, however, somewhat less for SP loading.

For LCB specimens, tested under CA and SP loading, there is no influence of yield strength on the fatigue strength. This behaviour was also expected, considering the results for small shear tensile specimens, tested under CA loading, in Fig. 1 [2]. It is probably the presence of crack-like defects in the weld region that cause an early start of crack propagation which in turn makes the fatigue strength independent of base metal strength.

The fatigue strength of LCB specimens made of stainless steel, 18Cr9Ni, are lower than those for other steel grades.

In cases when the fatigue life only consist of crack propagation the slope of the S–N curves, A_1, is related to the exponent, m, in Paris' law, as $A_1 = -m$.

The slopes A_1 for the S–N curves in this investigation are quoted in Table 6 for non-load carrying and load carrying beams.

For LCB specimens tested under CA loading $A_1 = -4.7$, when all steel grades, except 18Cr9Ni, are grouped together. This value is somewhat higher than the Paris' law exponent, $m = 3.42$–4.04, found from crack propagation tests [7] (Table 7). This indicates that the recorded fatigue life for steel grades MS, DP 600 and HSLA 350 might include a crack initiation phase.

Pulsating tension tests on spot welded specimens show that the fatigue life increases by adding a single overload to the CA loading. The increase in fatigue life was more pronounced in high strength steels and especially in those of dual-phase type [1].

Table 6. Constant A_1 in the S–N curves for non-load carrying and load carrying beams as tested

Steel grade	t (mm)	Loading condition	Load carrying beams A_1	Non-load carrying beams A_1
MS	1.0	CA	–6.504	–6.281
		OL	–6.762	—
DP 600	0.8	CA	–4.504	–5.863
		OL	–5.984	—
DP 600	1.0	CA	–4.352	–4.617
		OL	–3.700	—
HSLA 350	1.0	CA	–4.918	—
		OL	–5.452	—
18Cr9Ni	1.0	CA	–4.167	—
All steel grades except 18Cr9Ni		CA	–4.701	—

Table 7. Results from crack propagation tests, $R = 0.05$, thickness $t = 1.0$ mm

Steel grade	Constants in Paris' law $C \times 10^{-10}$	m	Threshold value ΔK_{th}	MPa$\sqrt{m}$
MS	1.36	4.04	6.6	(6.7, 6.2, 7.0)
DP 600	4.72	3.52	6.8	(6.8, 6.7)
HSLA 350	1.58	3.82	5.2	(5.1, 5.6, 4.7)

The results from LCB specimens tested with occasional overloads (Figs 5 and 7) confirm the positive effect of single overloads for grade DP 600. The increase in fatigue strength was 15–20%. For grade MS the increase was about 10%, while grade HSLA 350 shows no significant effect of overloads.

The increase in fatigue life caused by occasional overloads is normally explained by a retardation in fatigue crack growth rate following the overload. The increase in fatigue life, that follows the increase in base metal strength, can be related to a higher level of compressive residual stresses in the plastic zone in front of the crack. For DP steel crack deflection and roughness induced crack closure can also be a reason for longer fatigue life.

At $R = -1$ the compressive residual stresses introduced at the positive overload can be relaxed at the following negative overload. This can be a reason for less or no effect of overload appearing for grades MS and HSLA 350, respectively.

By the introduction of compressive residual stresses at overloads the effective stress intensity factor will be reduced. It is therefore reasonable to relate the fatigue strength at the overload tests to the threshold value, ΔK_{th}, of the steel. As can be seen in Table 7, the fatigue strengths at the overload tests (Table 5) are ranked in the same way as the threshold values.

The fatigue strength, S_{eq}, for LCB specimens tested under spectrum loading follow the same pattern as the overload test results as regards the influence of base metal yield strength (Fig. 7). This means that grade DP 600 show higher and grade HSLA 350 somewhat lower fatigue strength than grade MS. The fatigue strength of grade 18Cr9Ni, which was low when tested under Ca loading is now close to grade HSLA 350.

Influence of spectrum loading

The equivalent stress, S_{eq}, gives an idea of how well the fatigue strength under spectrum loading (SP) can be predicted by the Miner rule. Figure 7 shows that the SP results are lower than the constant amplitude (CA) results, i.e. a Miner rule prediction will be unconservative. The fatigue strength will be underestimated by about 25%.

The ratio between the maximum stress in the spectrum, S_{amax}, and the constant amplitude fatigue strength varies between 1.75 and 2.50 for different beam geometries and steel grades (Table 5). The spectrum used in this investigation represent a κ-value between 1/2 and 1/3 in the Swedish steel building code, BSK [8]. This value gives a ratio between SP and CA loading of 1.85–2.50, which is very close to what was found by the results from this investigation.

An actual Miner summation was also performed on all individual uncorrected SP results, however, without considering any fatigue limit, which makes the summation somewhat conservative. The Miner sum values for all grades are plotted versus the fatigue life in Fig. 8 and average values for different grades are shown in Fig. 9.

As can be seen in Fig. 8, the scatter is very large; however, considering Fig. 9 it looks as if the Miner sum is higher for load carrying beams in grade DP 600 and grade 18Cr9Ni. The very high value for 18Cr9Ni is associated with the very large difference in fatigue strength between CA and SP loading. One explanation can be a more pronounced strain hardening under SP loading compared to CA loading for grade 18Cr9Ni, which could result in higher compressive residual stresses and a lower effective stress intensity range.

The Miner sum is considerably lower than 1.0 for grade MS and HSLA 350, which means that a prediction of the fatigue strength under SP loading will be unconservative when using $\sum n_i/N_i = 1.0$. It is, however, not unusual that experiments can give a scatter in Miner sum between 0.3 and 3.

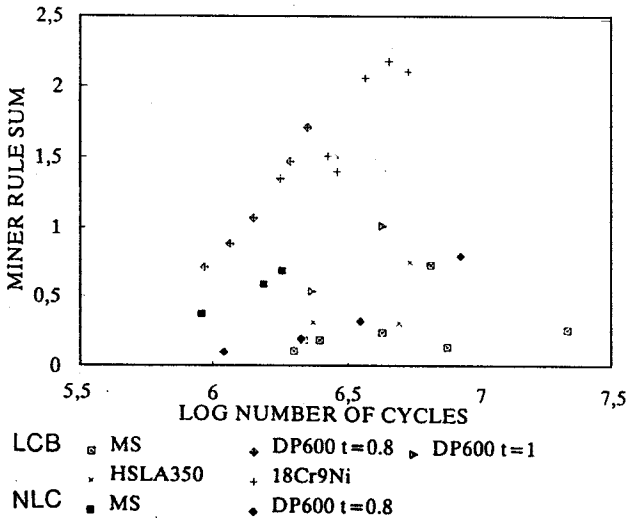

Fig. 8. Miner sum $\sum n_i/N_i$ for all individual results under spectrum loading

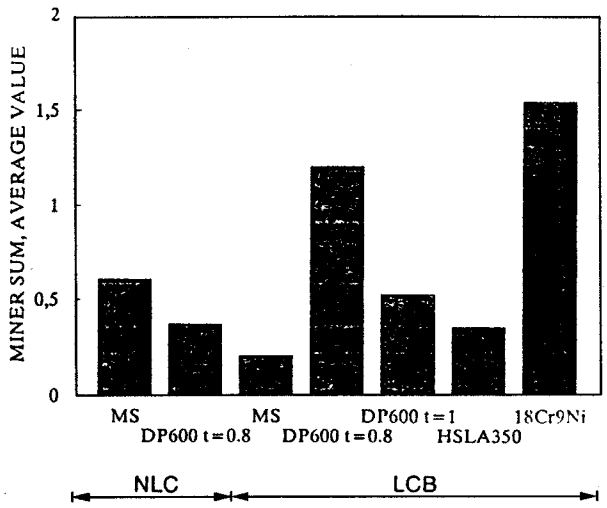

Fig. 9. Miner sum Σ_{ni}/N_i average values

Design and prediction models

There are very few methods existing for prediction of the fatigue behaviour of spot welded structures, and it is difficult to find a general method. The main design approach used in the industry today is to relate both the static strength and the fatigue strength to the nominal shear stress in the spot weld. There are, however, also other factors like the rotational stiffness, sheet thickness and tensile properties as well as the spot weld diameter, which give different levels of secondary bending stresses, which influence the fatigue properties.

In order to see whether there are ways of describing the fatigue behaviour of spot welded structures more in general some methods based on FE analysis, fracture mechanics, rotational stiffness and local stress approaches are tested on the experimental results in this and other investigations.

FE analysis

A linear elastic finite element analysis has been performed on load carrying beams with spot weld diameters 3, 4.2 and 6 mm and in sheet thicknesses 0.8 and 1.0 mm. Since the analysis of spot welds includes a singularity, the calculated stresses at the very circumference of the nugget will not be relevant. Instead, the stresses 1 mm outside the weld nugget are used for comparison. The FE model, being 1/4 of the specimen, is shown in Fig. 10. The load applied on the model is 500 N at each of the two loading points. This corresponds to a total load of 4000 N on a full beam, and a nominal bending stress of 84 MPa in the middle of the critical spot weld (weld 1 in Fig. 10), when the sheet thickness, t, is 1.0 mm.

The local tensile stress, S_x, on the outside surface of the inner beam is shown in Fig. 11 for a spot weld diameter of 4.2 mm. As can be seen in the figure, the stress has its maximum just outside the spot weld circumference, which is also observed being the point of crack initiation.

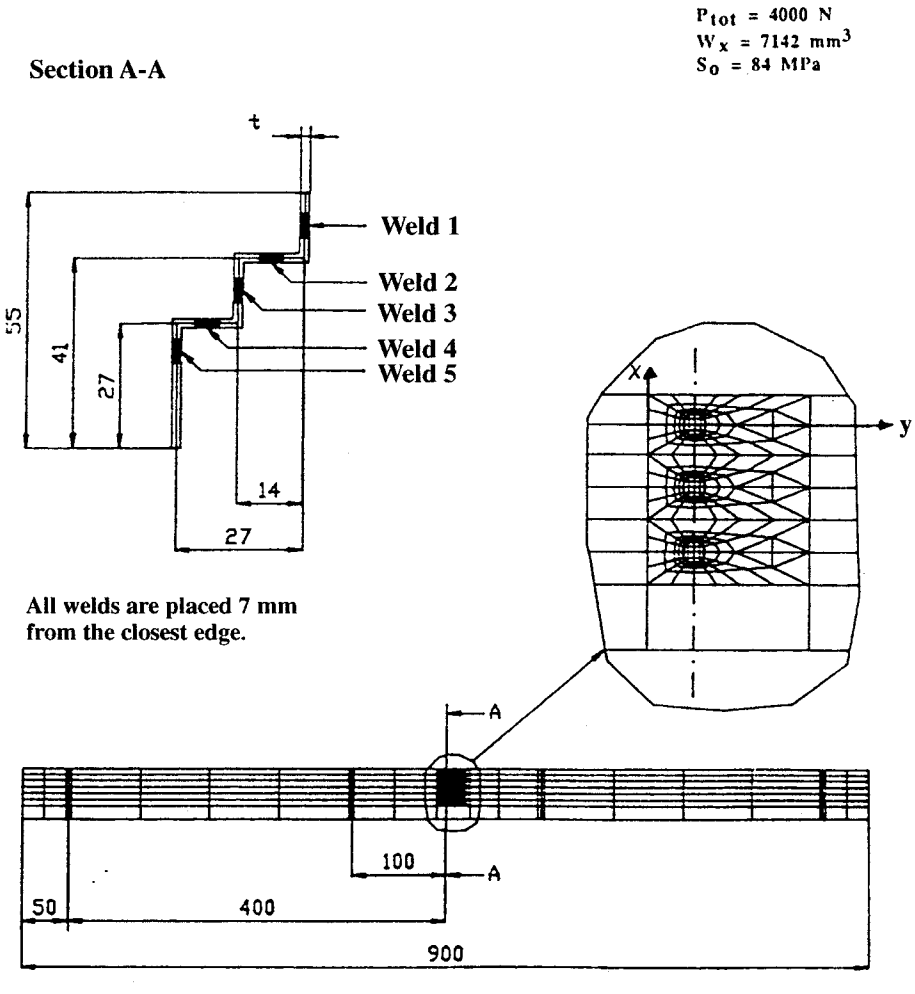

Fig. 10. FE model of spot welded load carrying beam (1/4), LCB

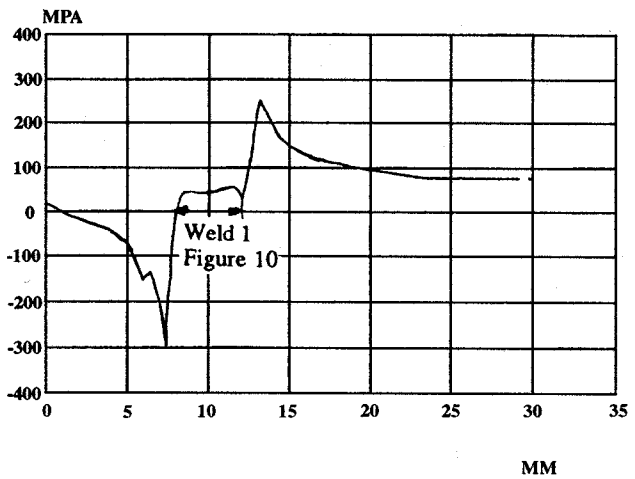

Fig. 11. Stress component S_x; inner beam outside, sheet thickness t = 1.0 mm, spot weld diameter d = 4.2 mm

The maximum tensile stress ($S_{x,max}$), the stress 1 mm outside the weld nugget ($S_{x,1\ mm}$), the maximum shear stress (τ_{max}), as well as the rotation of the weld (θ) are quoted in Table 8.

Additional results for other types of specimens

In order to get a broader basis for the evaluation of the prediction models experimental results from small specimens are also included in the analysis.

Fatigue tests have been performed on the shear tensile specimen with one spot weld (STS = *S*hear *T*ensile *S*ingle) [6, 9] or several spot welds in a row transverse the loading direction (STM = *S*hear *T*ensile *M*ultiple) [6, 9] as well as specimens with two spot welds in a row along the loading direction (STD = *S*hear *T*ensile *D*ouble) [4]. Specimen STS, STM and STD are shown in Figs 12(a), (b) and (c), respectively. These three specimens are asymmetrical and there will be additional bending stresses present in the critical site for fatigue crack initiation. In order to test a case where these secondary bending stresses are small a symmetrical shear tensile specimen with two spot welds (SST = *S*ymmetrical *S*hear *T*ension) [4] is also included. Specimen SST is shown in Fig. 12(d). Also a multispot H-shaped specimen (HST = *H*-shaped *S*hear *T*ension) [10] is included (Fig. 13).

The experimental fatigue strength results and the FE analysis results on local stresses, $S_{x,max}$ and $S_{x,1mm}$, and rotations, θ, are summarized for all specimens in Tables 9 and 10, respectively.

Fracture mechanics approach

Radaj [11] has made an attempt to find a relation between the fatigue strength of different spot welded joints by using a fracture mechanics approach. In this approach the stress intensity factors, K_I, K_{II} and K_{III}, are based on the local stress at the spot weld edge. In Fig. 14 [11] the fatigue strength is related to the equivalent stress intensity fact or, K_{eq}, for some of the specimens discussed here. The experimental values for the specimens are also included in Fig. 14. A comparison between the relations according to Radaj and the experimental values indicates that the fracture mechanical approach seems to be somewhat conservative. The symmetrical joint included by Radaj has one spot, while specimen SST has two spots. This could have given a stiffer joint and been in favour for the later joint, which show 50% higher fatigue strength than the one predicted by Radaj.

Table 8. Results from FE analysis on spot welded load carrying beams, nominal stress S_0 = 84 MPa

d (mm)	$S_{x,max}$ (MPa)	$S_{x,1\ mm}$ (MPa)	τ_{max} (MPa)	θ (deg)
3.0	330	300	227	0.163
4.2	250	240	160	0.117
6.0	185	175	110	0.076

The actual stress intensity range ΔK_I calculated by Radaj is recalculated to correspond to the fatigue strength level at $N = 10^6$ cycles and $R = 0$. This gives $\Delta K_I \approx 2.6$ MPa$\sqrt{m}$ for the specimens (STS, STM, HST) tested here that are free to rotate. This value is smaller than the threshold stress intensity factor found in this investigation (5.2–6.8 MPa$\sqrt{m}$). The reason for this can be that tensile residual stresses increase the effective stress intensity factor in the spot welded specimens compared to the crack propagation tests performed at $R = 0$. A recalculation to $R = 0.5$ gives Δk_{th} = 3.75 MPa$\sqrt{m}$ which is closer. Also the fact that the comparison only is made for ΔK_I, instead of ΔK_{eq}, could be an additional explanation of the difference.

Davidson stiffness approach

Davidson [12, 13] has proposed a relation between the fatigue properties and the elastic stiffness of the joint that is based on fracture mechanical consideration. He assumes that the separation between the sheets due to eccentric loading across a spot weld reflects the stress state at the crack tip during loading and can be correlated with CTOD, and hence with ΔK. Further, he assumes that the angle of rotation ($\Delta\theta_s$ and $\Delta\theta_N$ in Fig. 15) is proportional to the CTOD. ΔK is proportional to $\sqrt{\text{CTOD}}$, i.e. also to $\sqrt{\Delta\theta_s}$. The sheet separation (or rotation) reflects the response of the welded joints to nugget size, sheet thickness, weld arrangements and other factors. The limitations that exist in trying to analytically determine the stress intensity factor or the stress concentration factor to predict fatigue strength of spot welds can therefore according to Davidson, be circumvented by experimentally determining $\Delta\theta_N$.

The fatigue life can be estimated according to:

$$N = A\cdot(\Delta P\cdot\sqrt{\Delta\theta_N}/t)^{-3} \tag{3}$$

where

N = fatigue life (cycles)
A = constant = $1.84\cdot10^{15}$ (cycles·(N·$\sqrt{}$deg/mm)^3)
ΔP = fatigue load (N)
$\Delta\theta$ = angle of rotation at ΔP (deg)
t = sheet thickness (mm).

Adjusting the constant to $A = 4.4\cdot10^{13}$ give $N = 10^6$ cycles for the reference case, specimen STS. By applying this constant to the other specimens and calculate a predicted fatigue life we can get an estimate of the accuracy of the Davidson approach here. Along the same lines we can also predict a fatigue strength by using the relation $S_a \sim N^{-1/3}$. The results from that exercise are shown in Table 11. Considering Table 11 we see that the method seems to work for the specimens STS, STD and HST. For the specimens LCB and particularly SST with extremely little rotation the method is extremely unconservative.

Maddox local stress approach

Maddox [14, 15] has proposed a prediction method for spot welded shear tensile specimens based on a local stress, made up from

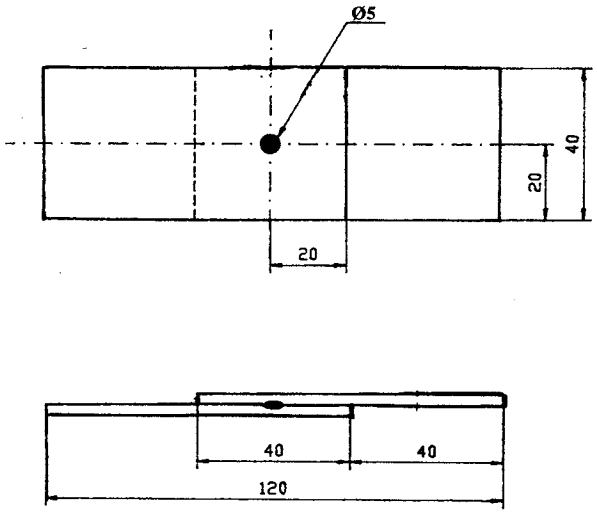

Sheet thickness 1 mm

a

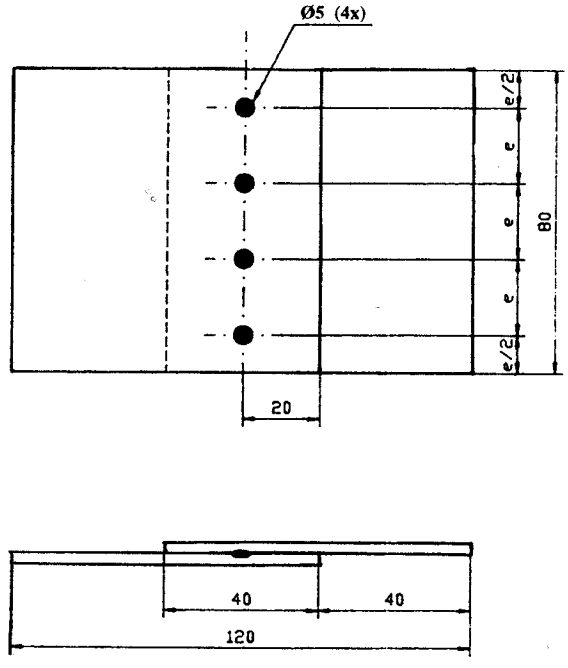

Sheet thickness 1 mm

b

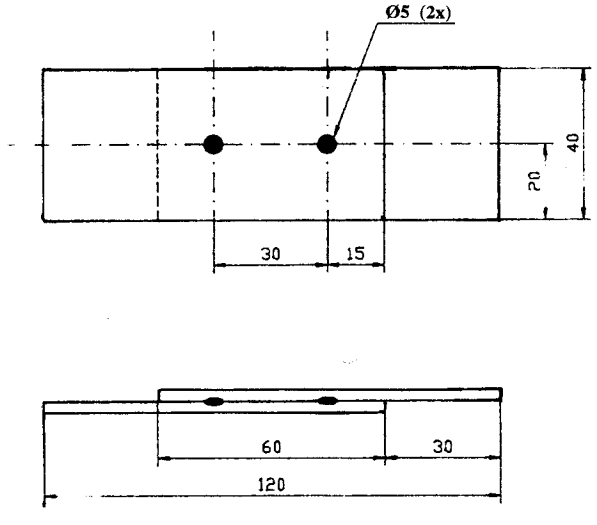

Sheet thickness 1 mm

c

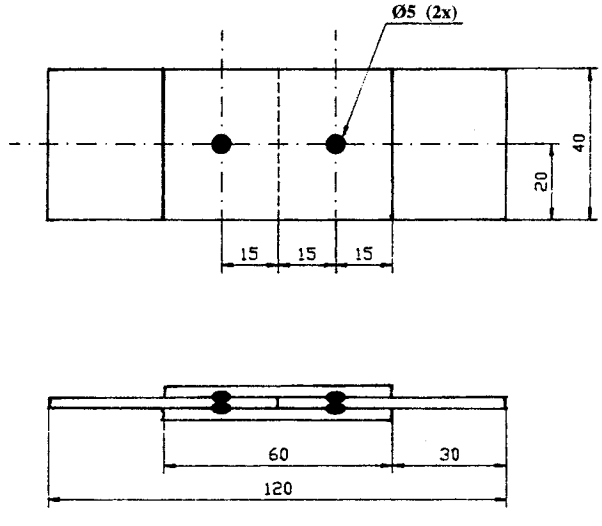

Sheet thickness 1 mm

d

Fig. 12. Small specimens used for additional tests: (a) STS = shear tensile single; (b) STM = shear tensile multiple; (c) STD = shear tensile double; (d) SST = symmetrical shear tension

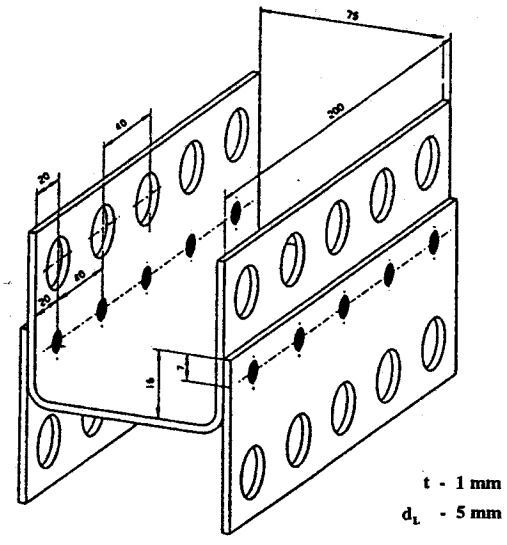

Fig. 13. The multispot H-shaped specimen (HST)

the local axial and bending stress components. He assumes that the axial stress acts uniformly around half the spot weld circumference and that the bending stress acts uniformly over the sheet width. The local stress at the spot weld can be calculated according to:

$$S_L = \frac{2 \cdot P_a}{\pi \cdot d \cdot t} + \frac{3 \cdot P_b}{e \cdot t} \qquad (4)$$

where

S_L = local stress (MPa)
P_a = axial load (N)
P_b = bending load (N)
d = spot weld diameter (mm)
t = sheet thickness (mm)
e = spot pitch (mm).

The load P for joints with more than one spot weld is taken as the load through each spot weld. For the multispot specimens (STM) the load used in the calculation is then $P_a = P_b = P/n$, where P is the total load and n the number of spot welds. For the load carrying beam (LCB) an integration of the shear stress over the spot weld cross section gives $P_a = P_b = 0.28 \cdot P$, where P is the total bending load on the beam.

The local stress amplitude, calculated according to Eq. (4), is shown in Fig. 16 for all individual test the results. For all specimens except for the load carrying beam (LCB) and symmetrical shear tension (SST) the results seem to fall within the same

Table 10. Results from FE analysis on spot welded specimens and beams; nominal stress S_0 = 100 MPa, thickness t = 1.0 mm, spot weld diameter d_0 = 5 mm

Specimen type	$S_{x,max}$ (MPa)	$S_{x,1\,mm}$ (MPa)	θ (deg)
STS	815	815	0.561
STD	665	584	0.385
SST	390	355	0.007
LCB	342	328	0.115
HST	—	776	0.600

SPECIMEN TYPE			
RADAJ	1	1.54	2.09
THIS INVESTIGATION	STS STM LCB HST 1.0 0.9 1.1 1.1	STD 2.1	SST 3.1

Fig. 14. Relations for the fatigue strength predicted from K_{eq} by Radaj and test results at $N = 10^6$ cycles presented in this report

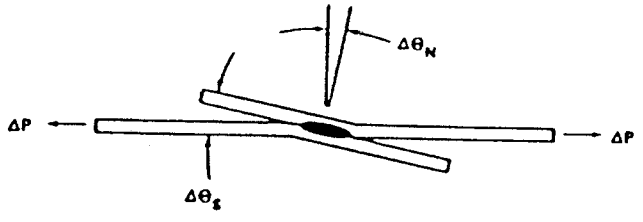

Fig. 15. Side view of a spot weld connection under tensile-shear loading showing the resultant sheet rotation, $\Delta\Theta_s$, and nugget rotation, $\Delta\Theta_N$, which occurs [12, 13]

Table 9. Summary of fatigue strength results on specimens and beams, recalculated to thickness t = 1.0 mm, spot weld diameter d_0 = 5 mm

Specimen type	$R = 0$		$R = 1$		Reference
	$S_{a,10^5}$ (MPa)	$S_{a,10^6}$ (MPa)	$S_{a,10^5}$ (MPa)	$S_{a,10^6}$ (MPa)	
STS	32.3	19.2	(40.4)	(24.0)	6, 9
STM	28.8	17.2	(36.0)	(21.5)	6, 9
STD	68.9	39.6	(86.1)	(49.5)	4
SST	77.5	59.4	(96.9)	(74.3)	4
LCB	(103.0)	(63.2)	128.8	79.0	4
HST	35.8	20.7	40.1	26.5	10

() calculated values acc. S_a ($R = -1$) = $1.25 \cdot S_a$ ($R = 0$).

Table 11. Predicted fatigue life and predicted and experimental fatigue strength using the Davidson approach, thickness $t = 1.0$ mm, spot weld diameter $d_0 = 5$ mm, $R = -1$

Specimen type	θ (deg)	Predicted fatigue life Number of cycles × 10^{-6}	Fatigue strength S_a at $N = 10^6$ cycles (MPa) Predicted	Experimental
STS	0.561	1.0 (ref)	24.0 (ref)	24.0
STD	0.385	0.544	40.4	49.5
SST	0.007	32.5	237.0	74.3
LCB	0.115	2.30	104.0	79.0
HST	0.600	0.581	22.1	26.5

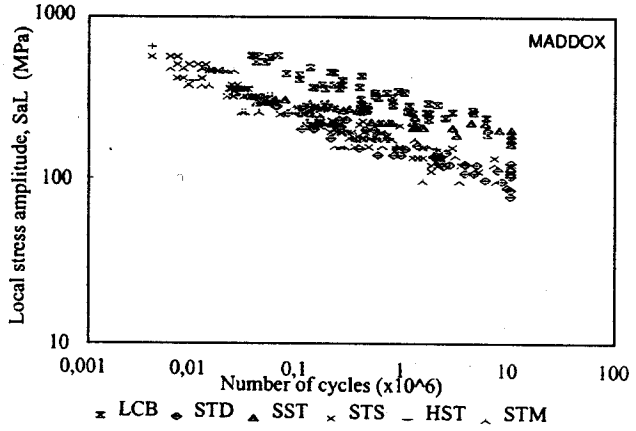

Fig. 16. Local stress calculated according to Maddox for different types of shear tensile specimens, $R = 0$

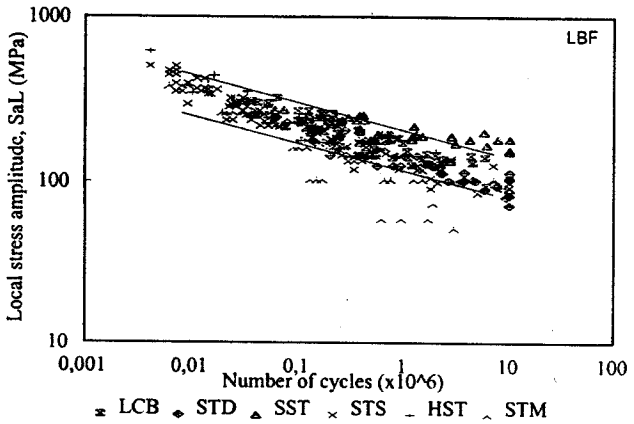

Fig. 17. Maximum local stress for different types of specimens calculated with the LBF method, $R = 0$

scatter band. In specimens LCB and SST the calculated local stress is considerably higher than for other specimens. This is probably due to the fact that the real bending stress is lower than the one calculated according to Eq. (4). Equation (4) is based on a free rotation of the spot weld (see Fig. 15), while in specimens LCB and SST the rotation is partly hindered. These results indicate that this method could predict the fatigue strength of shear tension spot welded structures fairly well in cases where the spot weld is free to rotate.

LBF local stress approach

LBF has proposed a method for predicting the fatigue strength of spot welded details based on a maximum local stress calculated by using cross sectional forces and bending moments at the centre of the weld [16]. This maximum local stress is calculated according to:

$$S_L = \frac{F_X}{\pi \cdot d \cdot t} + K \cdot 1.872 \cdot \frac{M_Y}{d \cdot t^2} \qquad (5)$$

where

S_L = maximum local stress (MPa)
F_X = load in the X-direction (N)
M_Y = bending moment in the Y-direction (Nmm)
$K = 0.6 \cdot \sqrt{t}$ = geometrical factor
d = spot weld diameter (mm)
t = sheet thickness (mm).

The maximum local stress amplitude, calculated according to Eq. (5), is shown in Fig. 17 for all individual test results presented in this investigation. In this figure the scatter band found by LBF [16] is also shown. As can be seen in the figure almost all test results fall within the LBF scatter band. Results from tests on the symmetrical shear tension specimens (SST) show somewhat higher local fatigue stresses at long life than the LBF scatter band, while some multispot specimens (STM) show lower local stresses. The slope of the S–N curve for specimen SST is, however, much shallower than for other specimens and some results at low fatigue lifes are below the line. A more thorough analysis shows that the STM specimens, which fall below the LBF scatter band, are those with very narrow spot pitch (e = 10 and 20 mm). With those exceptions the LBF prediction model seems to work very well.

Comparison of prediction models and practical implications

The accuracy with which the fatigue strength can be predicted has been summarized in Fig. 18. The relative predicted and experimental fatigue strengths are compared for the FE-model and models proposed by Radaj, Davidson, Maddox and LBF. For the model proposed by Davidson, the results for the relatively stiff joints, SST and LCB, are excluded. Values for specimen STM with spot pitches 10 and 20 mm are also excluded. The single spot shear tensile specimen (STS) has been chosen as a reference.

From Figure 18 it appears that the local stress approaches proposed by LBF and Maddox, give the best fatigue strength prediction for the shear joints included in this analysis.

In order to obtain an engineering tool for the design of shear loaded spot welded structures, a set of join classes, C, are recommended to be used for fatigue design. They are used for example in the Swedish code for fatigue design [8] and the Steel Sheet Handbook from SSAB Tunnplåt AB [17] which in turn is based on the IIW fatigue recommendation [18]. In those codes the joint class, C, is defined as the fatigue strength expressed as mean minus two standard deviations at $2 \cdot 10^6$ cycles. If the approaches

proposed by Maddox and LBF are used and the results in Figs 16 and 17 are analysed statistically we arrive at $C = 175$ and $C = 156$, respectively. The results for LCB specimens in Fig. 16 and STM specimens with spot pitches 10 and 20 mm in Fig. 17 are then excluded.

Conclusions

The results from this investigation can be concluded as follows:

- The fatigue strength of non-load carrying and load carrying beams expressed in terms of nominal tensile stress is almost independent of sheet thickness.
- The spot weld nugget diameter has a strong influence on the fatigue strength of load carrying beams. The fatigue strength is related to the nugget diameter as $S_d/S_{d0} = (d/d_0)^{0.8}$.
- The fatigue strength of non-load carrying beams increases along with increasing base metal yield strength.
- The fatigue strength for load carrying beams tested under constant amplitude loading is independent of base metal strength. This depends on the presence of crack-like defects in the weld region that cause an early start of crack propagation.
- The fatigue strength for load carrying beams in grade 18Cr9Ni is lower than for carbon steel when tested under constant amplitude loading, but about the same when tested under spectrum loading.
- Occasional overloads increase the fatigue strength for load carrying beams, especially in dual-phase steel.
- Load carrying beams in dual-phase steel also seems to have higher fatigue strength than other grades when tested under spectrum loading.
- The test results indicate that the Miner rule is unconservative. It underestimates the fatigue strength by about 25%.
- The Maddox and LBF local stress approaches seem to give the best prediction of the fatigue strength for the shear tensile joints tested here.
- When using the Maddox and LBF approaches we arrive at joint classes $C = 175$ and $C = 156$, respectively, according to the IIW fatigue recommendation.

Acknowledgements

The FE analysis was performed by Mats Olof Olsson and Jonas Bogren, The Aeronautical Research Institute of Sweden, and the crack propagation tests by Anna Hedlund-Åström and Bo Magnusson at the Department of Aeronautical Structures and Materials, Royal Institute of Technology. Their contributions to this investigation are greatly acknowledged. Thanks are due also to Professor Anders Blom at the same Institute for valuable discussions during the early stages of the investigation. The help in starting up the fatigue tests provided by Åke Lundin and others at Daltek Ab is also acknowledged. This project is a part of Eureka project 337, "New steels for automotive applications", which is run in cooperation with Hoesch Stahl, Audi AG, BAM Berlin, LBF and the Institute of Metals Research, Stockholm.

Good cooperation was also established with Avesta Sheffield AB during the project.

The project was financially supported by NUTEK (Swedish National Board for Industrial and Technical Development).

References

1. J.O. Sperle: Fatigue strength of spot welded high strength steel sheet. Swedish Symposium in Classical Fatigue, Sunne, Sweden, 29–31 January 1985.

2. J.O. Sperle: Fatigue strength of non-load carrying spot welds. WI-publ Metal Construction, Nov. 1984.

3. J.F. Cooper, R.A. Smith: Theoretical predictions of the fatigue life of shear spot welds. *Fatigue of Welded Constructions*, pp. 287–295, TWI, 1988.

4. J.O. Sperle, C. Lindgren, M. Jonsson: Fatigue strength of spot welded beams in high strength steels. Report No. HIFB-MC-HTM — 94/8, Materials Centre, HTM, University College of Falun/Borlänge.

5. H.G. Köbler: Generation of the standardized load sequence with Gaussian type frequency distribution of level crossings. LBF, Paper No. 5513/5517.

6. J.O. Sperle: Strength of spot welds in high strength steel sheet. *Metal Construction*, Vol. 15, No. 4, April 1983.

7. A. Hedlund-Åström, B. Magnusson: Determination of crack propagation data for MS, DP600 and HSLA 350 steel sheet. ILK Report 92-29, Department of Aeronautical Structures and Materials, Royal Institute of Technology, Stockholm, 1992.

8. Regulations for steel structures (in Swedish). Statens Planverk, Svensk Byggtjänst, 1987.

9. J.O. Sperle: Strength of spot welded joints — influence of nugget diameter and spot pitch. SSAB Tunnplåt AB, internal report 9/82 (in English).

10. Singh: Unpublished results/Eureka-project 337 — New steels in automotive applications.

11. D. Radaj: *Design and Analysis of Fatigue Resistant Welded Structures*. Abington Publishing, Cambridge, 1990 (ISBN 1 85573004 9).

12. J.A. Davidson, E.J. Imkof Jr: The effect of tensile strength of the fatigue life of spot welded sheet steel. SAE publ, No. 840110.

13. J.A. Davidson, E.J. Imkof Jr: A review of the fatigue properties of spot welded sheet steels. SAE publ, No. 830033.

14. S.J. Maddox: Fatigue design of welded structures. Engineering design in welded structures. IIW Conference Proc. Madrid, 7–8 Sept 1992.

15. S.J. Maddox: Fatigue behaviour of welded joints. Advances in Fatigue Science and Technology. NATO Advanced Study Institute, Portugal, April 1988.

16. A. Rupp, G. Grubisic: Ermittlung ertragbarer Beanspruchungen am Schweisspunkt auf Basis der übertragenen Schnittgrössen. To be published in 1994.

17. SSAB Sheet Steel Handbook. SSAB Tunnplåt AB, Sweden, 1991.

18. Design recommendations for cyclic loaded steel structures, IIW Doc-998-1981. *Welding in the World*, Vol. 20, No. 7/8, pp. 153–165, 1982.

Appendix I

This appendix contains all experimental results from fatigue tests on non-load carrying and load carrying beams.

Along with the fatigue test results, actual cross sectional data (W) of the beams as well as the measured spot weld diameter (d) of almost all individual beams are given (d^* = average value of diameters for beams welded at the same occasion). The different welding occasions have been given numbers.

Non-load carrying beams

Table A1(a). Results from tests with constant amplitude loading (CA)

Table A1(b). Results from tests with spectrum loading (SP)

Load carrying beams

Table A2(a). Results from tests with constant amplitude loading (CA)

Table A2(b). Results from tests with occasional overloads (OL)

Table A2(c). Results from tests with spectrum loading (SP)

Table A1(a). Primary fatigue test results on non-load carrying beams, constant amplitude loading (CA)

Steel grade	Specimen No.	Section modulus W (mm³)	Nugget diameter d (mm)	Welding occasion	Load F (kN)	Number of cycles $N \times 10^{-6}$	Stress S_a (MPa)
MS (A)	2	7347	4.45*	1	6.5	0.189	132.7
$t = 1.0$ mm	3	7347	4.70	1	6.5	0.194	132.7
	8	7347	4.45*	1	5.3	0.917	108.2
	9	7347	4.20	1	7.1	0.156	145.0
	10	7347	4.45*	1	7.1	0.137	145.0
	18	7347	4.45*	1	6.5	0.284	132.7
	19	7347	4.45*	1	6.5	0.400	132.7
DP 600	7	6004	4.18*	2	11.5	0.058	287.3
$t = 0.8$ mm	20	6004	4.18*	2	8.0	0.270	199.9
	21	6004	4.18*	2	7.0	0.682	174.9
	22	6004	4.18*	2	7.5	0.731	187.4
	23	6004	4.18*	2	11.5	0.028	287.3
	24	6004	4.10	2	7.5	0.356	187.4
	25	6004	4.25	2	7.5	0.591	187.4
DP 600	11	7347	5.24*	3	14.0	0.089	285.8
$t = 1.0$ mm	12	7347	5.24*	3	15.5	0.055	316.5
	14	7347	5.30	3	10.0	0.507	204.2
	15	7347	5.24*	3	10.0	0.454	204.2
	16	7347	5.18	3	10.0	0.306	204.2
	17	7347	5.24*	3	10.0	0.430	204.2
18Cr9Ni	196	8577	4.48*	11	9.0	0.221	157.4
$t = 1.0$ mm	198	8577	4.48*	11	8.8	0.414	153.9
	199	8577	4.48*	11	8.7	0.242	152.2

Table A1(b). Primary fatigue test results on non-load carrying beams, spectrum loading (SP)

Steel grade	Specimen No.	Section modulus W (mm³)	Nugget diameter d (mm)	Welding occasion	Load F (kN)	Number of cycles $N \times 10^{-6}$	Stress S_{amax} (MPa)	Stress S_{eq} (MPa)
MS (A)	155	8078	5.00*	3	12.0	6.414	222.8	75.9
$t = 1.0$ mm	158	8078	5.00*	3	12.0	1.786	222.8	92.0
	162	8078	5.00*	3	12.0	1.525	222.8	92.1
DP 600	156	6563	5.00*	3	12.0	1.098	274.3	111.6
$t = 8$ mm	159	6563	5.00*	3	12.0	2.120	274.3	111.6
	160	6563	5.00*	3	12.0	3.505	274.3	111.6
	161	6563	5.00*	3	12.0	8.341	274.3	111.6

Table A2(a). Primary fatigue test results on load carrying beams, constant amplitude loading (CA)

Steel grade	Specimen No.	Section modulus W (mm^3)	Nugget diameter d (mm)	Welding occasion	Load F (kN)	Number of cycles $N \times 10^{-6}$	Stress* S_a (MPa)
MS (A)	104	7918	4.80	4	3.5	4.300	68.5
$t = 1.0$ mm	105	7918	5.50	4	6.0	0.075	105.3
	106	7918	5.25	4	4.6	0.980	83.8
	107	7918	4.40	4	4.6	0.370	96.5
	108	7918	4.92*	4	4.6	0.866	88.3
	120	7868	4.25	5	4.5	0.134	97.7
	121	7868	4.40	5	4.5	0.177	95.0
	122	7868	4.28	5	4.5	0.138	97.2
	126	7868	4.22	5	3.0	5.800	65.5
	127	7868	4.30	5	3.0	2.400	64.5
MS (B)	148	7731	3.02*	5	4.0	0.211	116.2
$t = 1.0$ mm	149	7731	3.02	5	4.0	0.164	116.2
DP 600	37	6004	4.10	6	3.5	0.238	102.5
$t = 0.8$ mm	38	6004	4.00	6	3.0	0.385	89.6
	39	6004	4.18	6	5.5	0.041	158.6
	40	6004	4.09*	6	5.5	0.035	161.4
	41	6004	4.09*	6	5.5	0.036	161.4
	82	6004	4.89*	7	2.0	6.000	50.9
	89	6004	4.75	7	3.0	2.000	78.1
	128	6004	4.90	7	3.0	1.100	76.2
	130	6004	4.92	7	3.0	0.778	75.9
DP 600	30	7254	4.40	8	6.0	0.126	137.4
$t = 1.0$ mm	31	7254	4.27*	8	5.0	0.253	117.3
	32	7254	4.27*	8	7.0	0.062	164.2
	33	7254	3.90	8	4.5	0.257	113.5
	34	7254	4.38	8	4.0	0.756	92.0
	35	7254	4.60	8	7.0	0.052	154.7
	36	7254	4.45	8	4.0	0.562	90.8
	65	7254	5.18	9	3.5	2.800	70.4
	88	7254	5.42	9	3.5	1.700	67.9
	132	7254	5.35*	9	4.0	1.650	78.4
HSLA 350	69	7521	5.00	10	4.5	0.675	89.7
$t = 1.0$ mm	70	7521	5.10	10	6.0	0.197	117.8
	71	7521	5.30	10	3.5	4.453	66.6
	72	7521	5.42	10	7.0	0.039	130.9
	73	7521	5.40	10	7.0	0.047	131.3
	109	7521	5.20	10	6.0	0.211	116.0
	110	7521	5.05	10	4.5	0.520	89.0
	111	7521	5.62	10	4.5	0.527	81.7
	112	7521	5.88	10	6.0	0.384	105.1
	113	7521	5.47	10	3.5	1.190	65.0
	129	7521	5.30	10	3.5	1.600	66.6
18Cr9Ni	152	8588	3.65	11	5.0	0.099	112.3
$t = 1.0$ mm	153	8588	4.20	11	5.0	0.100	100.4
	154	8588	4.25	11	3.5	0.437	69.6
	163	8385	4.75	12	3.5	0.445	65.2
	164	8385	4.60	12	3.0	1.684	57.4
	166	8385	4.10	12	3.2	1.073	67.1

*Recalculated to $d = 5.0$ mm.

Table A2(b). Primary fatigue test results on load carrying beams, occasional overloads (OL)

Steel grade	Specimen No.	Section modulus W (mm³)	Nugget diameter d (mm)	Welding occasion	Load F (kN)	Number of cycles $N \times 10^{-6}$	Stress* S_a (MPa)
MS (B)	143	7731	3.05	5	4.0	0.275	115.3
$t = 1.0$ mm	144	7731	3.02*	5	4.0	0.250	116.2
	145	7731	3.00	5	4.0	0.100	116.8
	146	7731	3.02*	5	2.5	5.525	72.6
	147	7731	3.02*	5	3.0	0.800	87.1
DP 600	49	6004	4.89*	7	4.0	0.385	101.7
$t = 0.8$ mm	50	6004	4.89*	7	4.0	0.275	101.7
	51	6004	4.89*	7	4.0	0.294	101.7
	52	6004	4.75	7	3.5	1.850	91.1
	53	6004	4.80	7	3.5	3.750	90.3
	54	6004	4.89*	7	4.0	0.450	101.7
	55	6004	4.89*	7	5.0	0.100	127.2
	56	6004	4.89*	7	5.0	0.200	127.2
DP 600	47	7254	4.27*	8	6.5	0.135	152.5
$t = 1.0$ mm	48	7254	4.27*	8	6.5	0.150	152.5
	57	7254	5.13*	9	5.0	0.800	101.3
	58	7254	4.88	9	5.0	1.525	105.4
	59	7254	5.13*	9	5.0	0.400	101.3
	60	7254	5.13*	9	5.0	1.100	101.3
	61	7254	5.13*	9	4.5	3.150	91.2
	74	7254	5.00	9	5.0	1.320	103.4
	76	7254	5.13*	9	6.5	0.070	131.7
HSLA 350	75	7521	5.28*	10	7.0	0.050	133.7
$t = 1.0$ mm	77	7521	5.28*	10	5.0	0.275	95.5
	78	7521	5.28*	10	3.5	4.000	66.8
	79	7521	5.28*	10	5.0	0.525	95.5
	80	7521	5.28*	10	6.0	0.250	114.6
	114	7521	5.28*	10	3.5	1.650	66.8
	115	7521	5.28*	10	3.5	2.075	66.8
	116	7521	5.28*	10	5.0	0.225	95.5
	117	7521	5.28*	10	5.0	0.375	95.5
	118	7521	5.28*	10	5.0	0.350	95.5

*Recalculated to $d = 5.0$ mm.

Table A2(c). Primary fatigue test results on load carrying beams, spectrum loading (SP)

Steel grade	Specimen No.	Section modulus W (mm³)	Nugget diameter d (mm)	Welding occasion	Load F (kN)	Number of cycles $N \times 10^{-6}$	Stress* S_{amax} (MPa)	Stress* S_{eq} (MPa)
MS (A)	102	7918	4.72	4	6.0	21.032	119.0	51.0
$t = 1.0$ mm	103	7918	4.50	4	6.0	7.461	123.7	55.7
	124	7868	4.15	5	6.0	2.165	132.8	58.4
	125	7868	4.28	5	6.0	2.484	129.5	57.0
	133	7918	5.30	4	6.9	4.230	124.8	56.2
	134	7918	4.92*	4	6.9	1.992	132.4	55.8
DP 600	135	5979	4.80*	7	6.9	1.900	178.8	68.6
$t = 0.8$ mm	136	5979	4.80*	7	6.9	1.144	178.8	68.1
	137	5979	4.80*	7	6.9	1.389	178.8	64.4
	138	5979	4.80*	7	6.9	1.750	178.8	68.2
	139	5979	4.80*	7	6.9	0.926	178.8	68.2
	140	5979	4.80*	7	6.9	2.206	178.8	68.2
DP 600	93	7299	5.13*	9	7.5	2.320	151.0	58.1
$t = 1.0$ mm	94	7299	5.15	9	7.5	4.220	150.5	58.2
HSLA 350	99	7521	5.28	10	7.0	2.345	133.7	52.5
$t = 1.0$ mm	100	7521	4.95	10	7.0	5.344	140.7	55.3
	101	7521	4.98*	10	6.0	4.885	120.0	47.2
18Cr9Ni	168	8385	4.48*	12	7.2	5.198	140.6	49.5
$t = 1.0$ mm	169	8385	4.48*	12	6.9	2.841	134.8	51.5
	170	8510	4.48*	13	7.0	4.405	134.7	51.5
	192	8510	4.48*	13	7.2	3.589	138.6	52.9
	195	8510	4.48*	13	7.2	2.624	138.6	52.9

*Recalculated to $d = 5.0$ mm.